

# Pulse-mode operation of high-frequency power supplies for ESPs

Per Ranstad  
Alstom Power  
Sweden  
per.ranstad@  
power.alstom.com

Anders Karlsson  
Alstom Power  
Sweden  
[anders-electro.karlsson@  
power.alstom.com](mailto:anders-electro.karlsson@power.alstom.com)

Lena Lillieblad  
Alstom Power  
Sweden  
lena.lillieblad@  
power.alstom.com

## Abstract:

High-frequency power supplies were originally introduced on the ESP market in 1993 (ALSTOM/SIR). Initially the high frequency power supplies were most often installed on low- to medium-resistivity applications due to limited power capabilities. During the last years more powerful models have been introduced, which are suitable for utility installations. In many cases these are burning coals, which produces a high resistivity flyash.

When applying high-frequency power supplies (HFPS) to high-resistivity dust applications, pulsed mode operation needs to be applied in order to avoid back corona. It is the objective of this paper to present pulsed mode operation of HFPS. Different aspects, such as: pulse parameters, spark-overs, and the resulting ESP-voltage and -current waveforms will be discussed. Results from power-plant (coal) installations are presented.

## 1 Introduction

High-frequency power supplies were originally introduced on the ESP market in 1993 [1]. An evaluation of the experiences gained during the first decade of operation was presented in [2].

When applying high-frequency power supplies (HFPS) to high-resistivity dust applications, pulsed mode operation is called for in order to avoid back corona [3], [4]. It is the objective of this paper to present pulsed mode operation of HFPS. Different aspects, such as: pulse parameters, spark-over, and the resulting ESP-voltage and -current waveforms will be discussed. Results from power-plant (coal) installations will be presented.

A general description of the basic operation on a fundamental operation of an ESP is presented in Fig 1. The flue gas is made to pass between two electrodes, the discharge

electrode (DE) and the collecting electrode (CE). A high DC voltage is applied to the electrodes, typically so that the CE is connected to ground and the DE to a negative potential (20-150 kV). The high electrical field close to the DE initiates a corona discharge, i.e. negative charges are emitted from the DE.

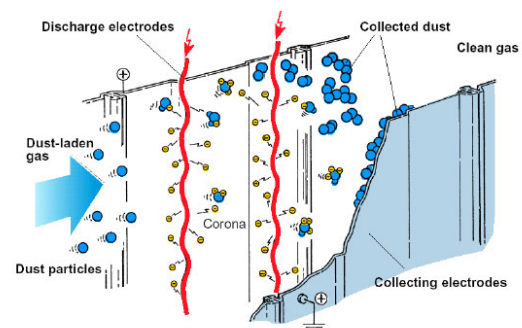


Fig. 1: Electrostatic dust precipitation

The negative charges will drift towards the positive electrode, CE. Some of the charges will stick to particles and make

these to drift in a similar way towards the CE. The collected dust is dislodged by means of mechanical rapping or by spraying water.

The electrical characteristic of an ESP bus-section is given by the energy storage in the electrical field and the corona discharge. Fig. 2 indicates the corona discharge characteristic, i.e. the VI-curve [5]. From the diagram the non-linear characteristic is clearly indicated. Below a threshold voltage,  $U_{onset}$ , no corona current is present. However, above  $U_{onset}$  the current will increase with an increasing voltage, steeper at higher voltages. The operation is limited by the spark-over voltage,  $U_{spark}$ . In Fig. 3 an equivalent circuit of the bus-section is shown. The capacitance,  $C$ , represents the energy stored in the electrical field. The diode,  $D$ , and the non-linear resistance,  $R$ , represent the corona discharge characteristic.

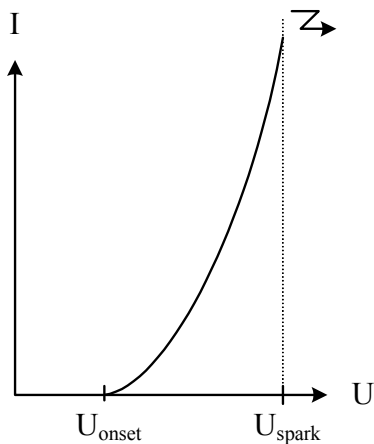


Fig. 2: Electrical characteristic, VI-curve

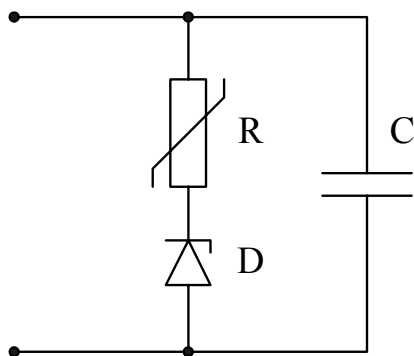
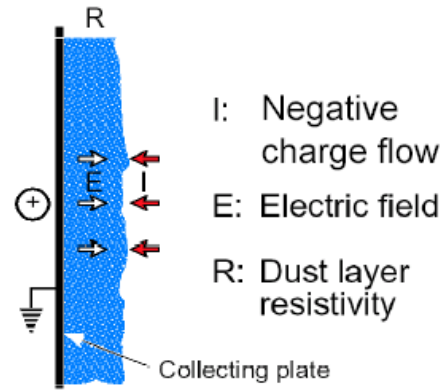
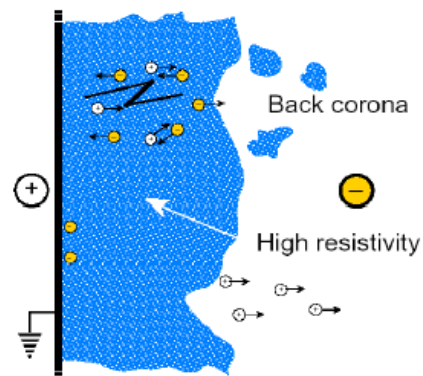


Fig. 3: Electrical characteristic, equivalent circuit

From Fig. 1 is also observed that the corona charges have to pass through the dust-layer in order to reach the CE. Fig. 4 shows the dust-layer in a more detailed view.



(a)



(b)

Fig. 4: Dust layer; (a) General, (b) High resistivity dust.

Fig. 4(a) shows the general case where the flow of negative charges form an electrical field in the dust-layer. The field strength,  $E$ , is given by the current density,  $J$ , and the dust-layer resistivity,  $R$ , as

$$E = J \cdot R. \quad (1)$$

In a situation where the dust resistivity, Fig. 4(b), is comparably high, back-corona may occur, i.e. the field strength in the dust-layer is high enough to cause local spark-over, which injects positive charges into the gas stream [5]. The positive charges recombine with the negative charge from the DE. Consequently, the collecting efficiency is reduced and the power consumption is increased. Fig. 5

indicates the collecting efficiency as a function of input power for back-corona and non-back-corona conditions, respectively. The diagram shows that in the case of back-corona the emission will start to increase if the power is increased above a certain level. In the case of non-back-corona operation the emission is decreasing for an increased power input.

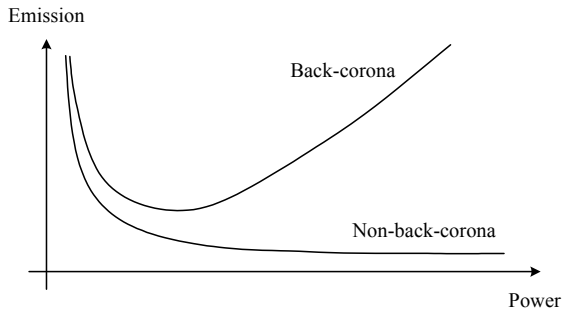


Fig. 5: Dust emission vs input power

In order to reduce the negative effects from back-corona, the corona current has to be reduced. This is preferably achieved by pulsed mode operation. Fig. 6 shows the current input in pulsed mode operation.

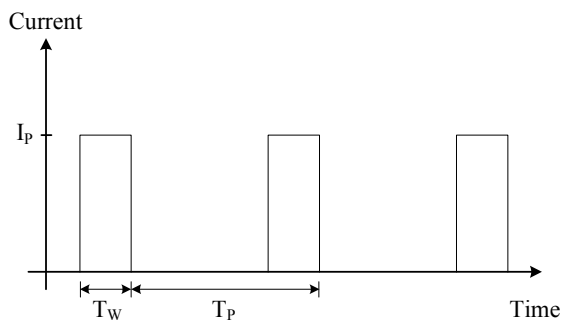


Fig. 6: Idealized current waveform

Since the average current is kept at a low level in pulse mode operation the back corona is limited. However, the high peaks of the current ensure an even current distribution over the DE, which improves the collecting efficiency.

Two different types of power supplies dominate the installed base of ESPs, Fig. 7. The line frequency power supply is shown in Fig. 7(a). A single-phase voltage is supplied to a pair of anti-parallel thyristors, which are connected in the primary circuit of a high-voltage transformer. The secondary winding of the transformer is connected to a diode rectifier. The DC-output of the rectifier is connected to the DE of an ESP bus-section. The high voltage transformer and the output rectifier are

commonly housed in an oil-filled vessel and is referred to as a T/R-set. The voltage and current of the ESP are sensed by a controller, which controls the conduction angle of the thyristors. This setup of the power supply was established in the 70ies when the power thyristor was introduced.

More recently the high frequency power supply (HFPS) has been introduced, Fig. 7(b). The first commercial installations were made 1993 and the original publication [1] was presented in Toronto, Canada in 1995. The major difference compared to the mains frequency power supply is the much higher operational frequency, 25-50 kHz vs 50/60 Hz. The HFPS is fed from the three phase mains. The input voltage is rectified and supplied to a transistor-bridge configuration. The transistors are turned on and off in a sequence so that the required high frequency voltage is applied to the transformer primary. The secondary of the transformer is rectified and connected to the ESP.

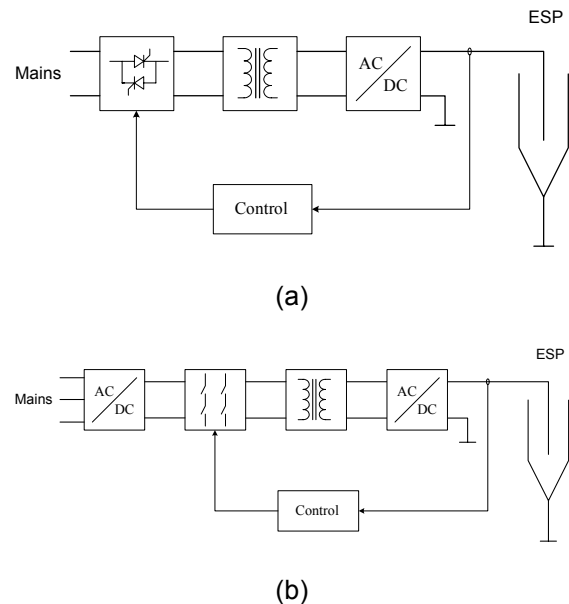


Fig. 7: Block diagrams of ESP power supplies; (a) Line frequency, (b) High frequency

Fig. 8 compares the ESP voltages obtained when energized from a line frequency power supply and a high frequency power supply, respectively [1].

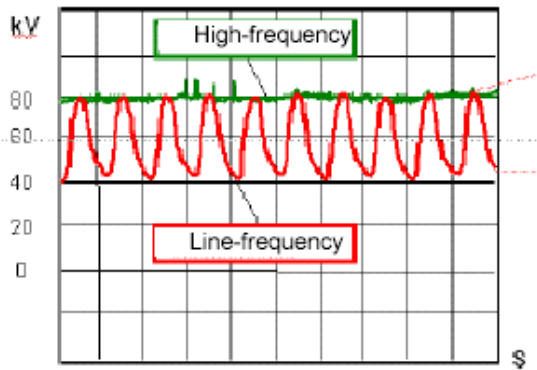


Fig. 8: Voltage ripple; line frequency power supply and high-frequency power supply

As a consequence of the almost ripple free voltage, in the case of HFPS energization, more current can be supplied to the ESP. The higher corona current and the increased average voltage will improve the collecting efficiency, in the case of non-back-corona conditions, Fig. 5. In the case of back-corona conditions the power supply is operated in pulsed mode, Fig. 6.

The most commonly used topology for HFPS on ESPs, the series loaded resonant (SLR) converter is shown in Fig. 9 [6]. It is estimated that more than 90 % of the installed fleet of HFPS is using this topology or derivatives thereof.

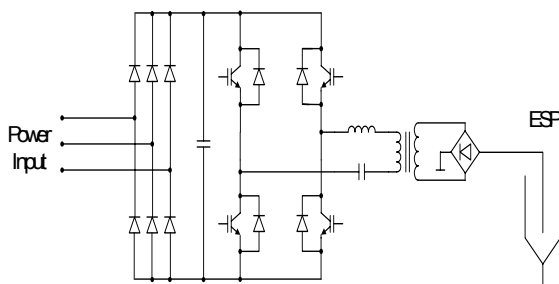


Fig. 9: Main circuit diagram, HFPS

The circuit contains a full bridge three-phase input rectifier followed by DC-link capacitor. The DC-link voltage is converted into a high-frequency voltage by means of an H-bridge (IGBT-inverter). The output of the H-bridge is connected to the primary of the high-frequency high-voltage transformer via a resonant tank. The purpose of the resonant tank is to control the switching losses by means of soft-switching. The transformer secondary is

connected to a high-voltage rectifier which supplies the output current to the ESP. Representing the HFPS by a current source, as shown in Fig. 10, indicates the pulsating output current,  $i_o$ , which is fed from the power supply to the load.

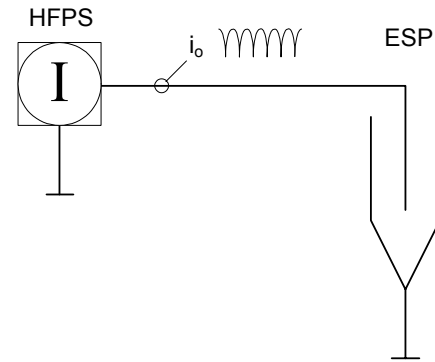


Fig. 10: Electrical system

Introducing the equivalent circuit of the ESP, Fig. 3, into the system, Fig. 10, results in the circuit shown in Fig. 11.

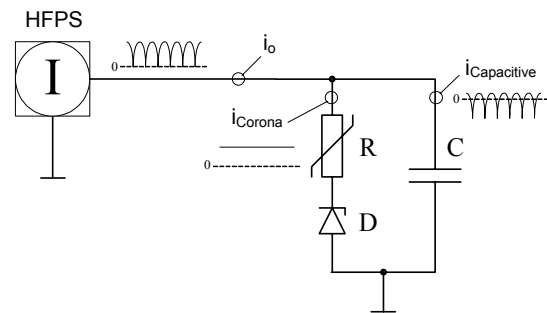


Fig. 11: Equivalent circuit

From the figure it is found that  $i_o$  may be subdivided into two components  $i_{Corona}$  and  $i_{Capacitive}$

$$i_o = i_{Corona} + i_{Capacitive} \quad (2)$$

where  $i_{Capacitive}$  consists of the AC-component of  $i_o$  and  $i_{Corona}$  represents the DC-component of  $i_o$ , as indicated in Fig. 11. The capacitive current is given by

$$i_{Capacitive} = C \cdot \frac{du}{dt} \quad (3)$$

The corona discharge current can be estimated by using

$$i_{Corona} = k \cdot (u - U_{Onset})^2 \quad (4)$$

where  $u$  is the ESP voltage and  $k$  is a constant.

Utilizing (2) and some typical parameters from an ESP operation ( $I=1\text{ A}$ ,  $U=50\text{ kV}$ ,  $C=100\text{ nF}$ ,  $f=30\text{ kHz}$ ), the voltage ripple,  $\Delta U$ , from the high-frequency component  $i_o$  may be estimated as

$$\Delta U \approx \frac{1}{4 \cdot 30 \cdot 10^3 \cdot 100 \cdot 10^{-9}} V \approx 80V.$$

Normalizing,  $\Delta U$ , to the load voltage yields the relative ripple voltage,

$$\Delta U' \approx \frac{80}{50 \cdot 10^3} = 0,16\%, \text{ which shows that}$$

the capacitance of the ESP acts an almost perfect filter for the high-frequency current component.

It should be noted that only  $i_o$  can be measured,  $i_{Corona}$  and  $i_{Capacitive}$  are present inside the ESP only and can not be measured separately.

## 2 Pulsed mode operation

In pulsed mode operation the converter is operated in an intermittent mode, i.e. the H-bridge is operated during the time of the current pulse time,  $T_w$  (Fig. 6), and paused during the remaining part of the period,  $T_p - T_w$  (Fig. 6). Figs. 12-15 present measurements in pulsed mode operation from an ESP down stream a 210 MW<sub>e</sub> coal-fired boiler. Fig. 12 shows the load (ESP) voltage and current. The load current is filtered in order to not display the high-frequency component.

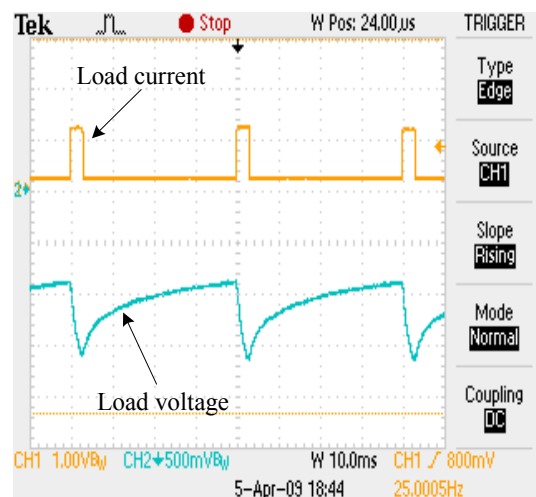


Fig. 12: Pulsed mode operation, (10 ms/div)

Fig. 13 displays the waveforms in a more detailed time scale during the current pulse,  $T_w$ . It also adds the primary current of the transformer, which clearly indicates the operation of the H-bridge during  $T_w$ . Fig. 14 displays the traces at a time resolution where also the individual cycles of the primary current can be observed.

During the pulse,  $i_o = I_p$ , the load voltage increases and consequently the corona discharge becomes more intense, as indicated in (4). During the pause,  $i_o = 0$ , the energy stored in the capacitance will be discharged by  $i_{Corona}$  causing the voltage decay.

Since the corona discharge current depends on the instantaneous value of the voltage across the electrodes (4), it is evident that the corona current will flow not only during the current pulse but also during the pause, caused by the energy storage of the capacitance.

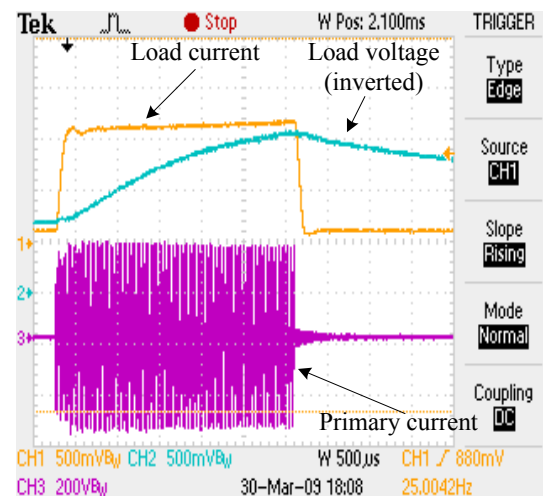


Fig. 13: Measured waveforms, (0,5 ms/div)

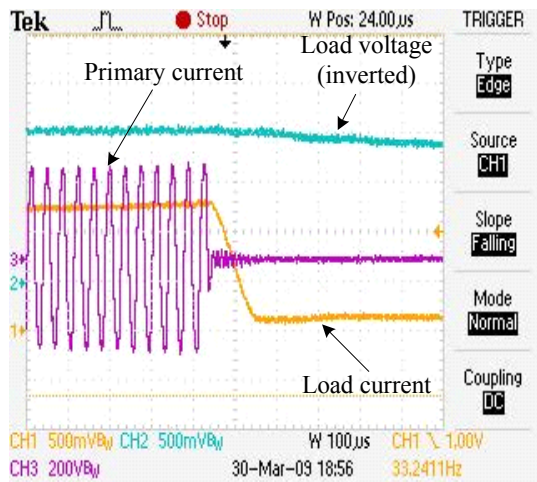


Fig. 14: Measured waveforms, (0,1 ms/div)

In Fig. 15, the waveforms at the occurrence of a spark-over are displayed. The load voltage shows a fast decay and the reaction time for the system to interrupt the power input is less than half a period of the conversion frequency, i.e.  $<20 \mu\text{s}$ . The peak, seen on the load current during the decay of the voltage originates from the discharge of the winding capacitance of the high voltage transformer caused by the spark-over.

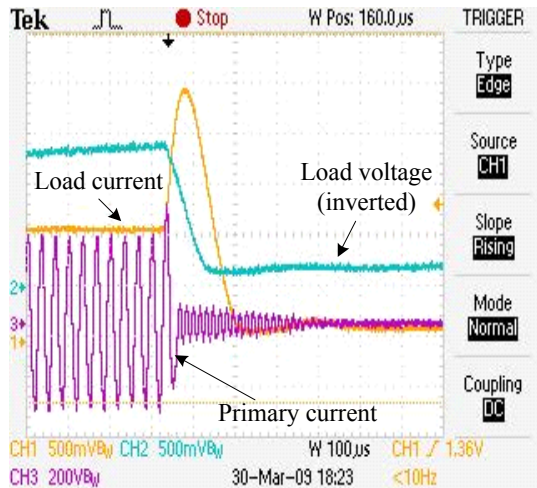


Fig. 15: Measured waveforms, spark-over (0,1 ms/div)

### 3 Conclusion

A general analysis of the operation of HFPS in continuous mode including an electrical model of the ESP has been presented. The voltage ripple originating from the high-frequency current component has been estimated and found to be very low,  $< 0,2\%$ .

The pulsed mode operation has been analysed, including the influence from the electrical characteristic of the ESP. It is

explained how the corona discharge current differs from the current pulse supplied to the ESP. The pulse mode operation is discussed based on measurements from a 210 MWe coal fired boiler.

### 4 Literature

- [1] P. Ranstad and K. Porle, "High frequency power conversion: A new technique for ESP energization", Proceedings of the EPRI/DOE International Conference on Managing Hazardous and Particulate Air Pollutants, Toronto, Canada, August 1995.
- [2] P. Ranstad, C. Mauritzson, M. Kirsten, R. Ridgeway, "On experiences of the application of high-frequency power converters for ESP energisation, " Proceedings of the 9<sup>th</sup> International Conference on Electrostatic Precipitation, ICESP IX, Mpumalanga, South Africa, May 2004.
- [3] H. Jacobsson, M. Thimansson, K. Porle, and M. Kirsten, "Back-Corona Control with help of Advanced Microprocessor Enhances Performance, " in Proc. of ICESP VI, Budapest, Hungary, June 1996.
- [4] C. S, Deye, C. M., Layman; "A Review of Electrostatic Precipitator Upgrades and SO<sub>2</sub> Reduction at the Tennessee Valley Authority Johnsonville Fossil Plant"; Power Plant Air Pollutant Control "Mega" Symposium; 2008
- [5] K. R., Parker; "Applied electrostatic precipitation"; Blackie Academic & Professional; ISBN 0 7514 0266 4; 1997
- [6] P. Ranstad, "Design and Control Aspects on Components and Systems in High-Voltage Converters for Industrial Applications, " PhD Thesis, Royal Institute of technology, Stockholm, Sweden, Oct 2010.